

REVIEW AND OPERATION OF SINGLE-PHASE RECONFIGURABLE INVERTER TOPOLOGY FOR A SOLAR POWERED HYBRID AC/DC HOME

Ajhar Shaikh¹, Prof. Mayuri Prajapati²

¹PG Scholar, ²HOD, E.C Department, KITRC, Kalol, Gandhinagar, Gujarat, India

Abstract: In this paper modelling, simulation and control of grid tie PV system using multilevel inverter are described. The majority of PV systems require inverters as interfacing units. A reconfigurable single phase inverter topology for a hybrid ac/dc solar powered home is suggested here. This inverter possesses a single-phase single-stage topology and the main advantage of this converter is that it can perform dc/dc, dc/ac, and grid tie operation, thus reducing loss, cost, and size of the converter. This hybrid ac/dc home has both ac and dc appliances. This type of home helps to reduce the power loss by avoiding unnecessary double stages of power conversion and improves the harmonic profile by isolating dc loads to dc supply side and rest to ac side. Simulation is done in MATLAB/Simulink and the obtained results are validated through hardware implementation using Arduino Uno controller. Such type of solar powered home equipped with this novel inverter topology could become a basic building block for future energy efficient smart grid and micro grid.

I. INTRODUCTION

Due to increasing power demand many new alternatives of power generation are used effectively. Out of all these photovoltaic generation is effective and can easily be implemented. The power from the PV system have different outputs depending on the condition of temperature and irradiance. To extract maximum power from PV array different MPPT algorithms are available such as, perturb and observe (P&O), incremental conductance (INC) and many more. Out of all these INC have some advantages and commonly implemented in many PV applications. This mppt controller is used to extract maximum power under all the irradiance conditions using boost converter. The output of PV system serves as DC link for the inverter. A power controlling method is employed to synchronize the PV system with grid. Generally, there are 2 main power stages in a grid tie PV system. First is DC link voltage control stage that maintains constant DC link voltage across inverter input and second stage consist of inverter current control that controls the current injected into the grid. Current control can be employed in many reference frames such as, stationary reference frame (α - β), synchronous reference frame (d-q) and natural reference frame (a-b-c). In the proposed system synchronous reference frame is employed using proportional integral (PI) controller.

II. SOLAR PHOTOVOLTAIC ARRAY

The Solar Photovoltaic Array is formed by connecting several solar panels in series and parallel combination to

generate the required power. The smallest component of the solar photovoltaic array is called photovoltaic(PV) cell. The ideal solar photovoltaic cell is represented by the equivalent circuit shown in Fig 1. These cells are connected in series of 36 or 72 cells to form one module. Similarly, several modules are assembled into a single structure to form array. Finally, assembly of these photovoltaic arrays are connected in parallel to obtain the required power. In PV module, series resistance (R_s) is comparatively more predominant and R_{sh} is considered equal to infinity ideally. The open circuit voltage(V_{oc}) of the PV cell is directly proportional to solar irradiation and V_{oc} is inversely proportional to the temperature.

The PV Array is characterised based on the I-V and P-V characteristic. As we can see from Fig.2 and Fig. 3,the variation in irradiation result variation in the current and the curves of I-V characteristic vary largely for different level of irradiation. The irradiation directly affects the PV Array current while the change of temperature directly affects the voltage generated by the PV Array as shown in Fig. 4 and Fig. 5. So same observation we can made from the below graphs of I-V and P-V characteristics at different irradiation and temperature level.

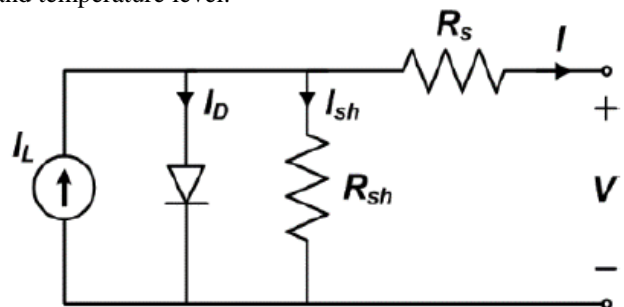


Figure 1: Equivalent circuit of PV cell

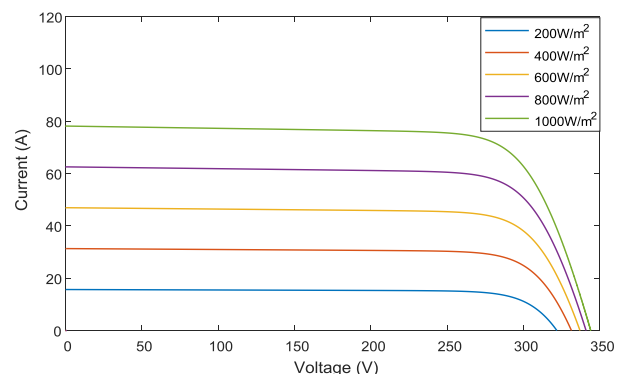


Figure 2: I-V characteristics of 20kW PV Array at different irradiation levels

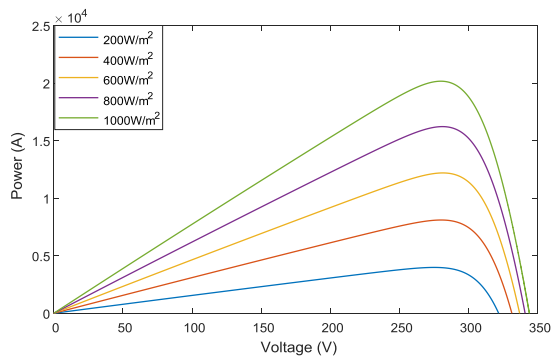


Figure 3: P-V characteristics of 20kW PV Array at different irradiation levels

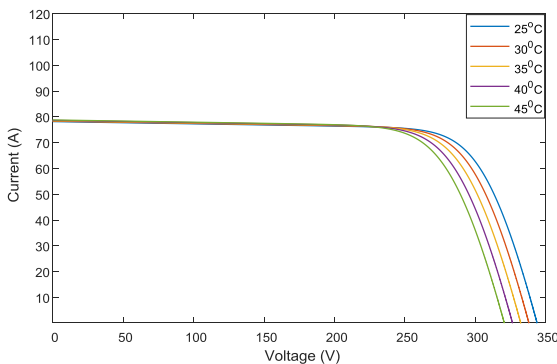


Figure 4: I-V characteristics of 20kW PV Array at different temperature levels

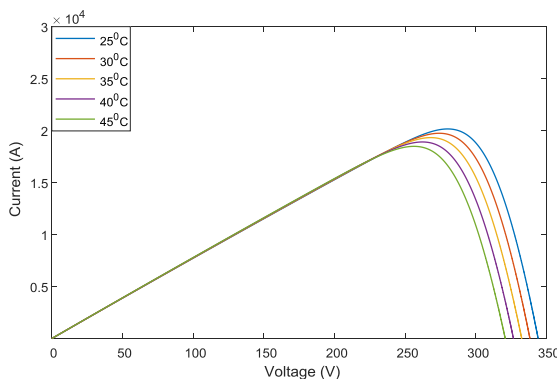


Figure 5: P-V characteristics of 20kW PV Array at different temperature levels

Single-Stage Solar PV Inverter for Small-Scale Systems

Compared to the single-stage one, the multistage power conversion is somewhat more expensive and affects the efficiency of the PV inverter. To reduce the volume and weight as well as the power conversion loss and cost, a hybrid PV battery-powered DC bus system was proposed in 2009 [2]. The DC to AC conversion stage-less DC bus system is very applicable to electronic equipment and appliances with high system efficiencies. The PV-battery-powered DC bus system is shown in Fig. For AC systems, a single-stage PV inverter was proposed in [2], and the circuit topology of single-stage inverter is shown in Fig. The proposed inverter performs a dual function: MPPT and outputting a sinusoidal current, which makes the control circuit complex. In [2], an alternative control technique was

developed to reduce the complexity of the control circuit. However, the common-mode issue was not considered in the proposed single stage inverter systems. The neutral point clamped (NPC) converter topology has the opportunity to connect the grid neutral point to middle point

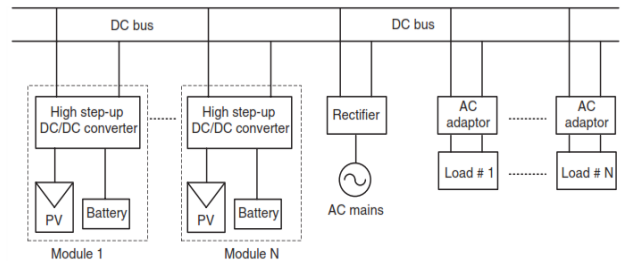


Fig PV-battery-powered DC bus system [2]

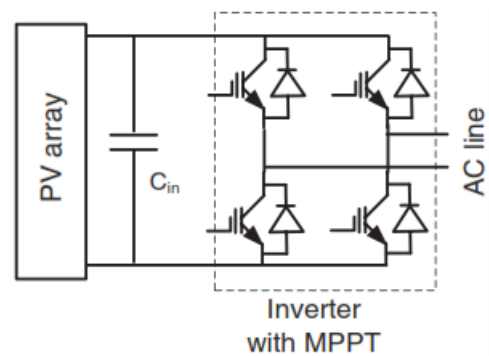


Fig Full-bridge with MPPT-based circuit topology of single-stage inverter [2]

Of the DC link, reducing the ground leakage currents. In this context, an NPC topology-based single-phase PV inverter as shown in Fig. was presented in [3] and a three phase PV inverter system in Fig. was implemented in [3]. Since the presented circuits are run as buck converters, the PV array voltages should be greater than the peak values of the output AC voltages. If V is the inverter output AC voltage and R is the reservation factor, the minimum array voltage can be calculated as

$$V_A = \sqrt{2}V_{rms}R. \dots (1)$$

Therefore, a few PV arrays in series connection are necessary to obtain the desired voltage. From the available literature, several single-stage topologies have been proposed based on either boost or buck–boost configurations. An integrated (boost converter and full-bridge inverter) PV inverter circuit topology shown in Fig. was presented in [3]. The output power quality and the efficiency of the inverter are limited by the fact that the boost converter cannot generate the output voltage lower than the input voltage. A universal single-stage PV inverter shown in Fig. was presented in that can operate as a buck, boost, or buck–boost converter. This inverter can operate with a wide range of input voltage, improving the power quality and the efficiency. Using the integrated buck–boost and inversion functions, several modified configurations have been presented in [3]. However, these topologies are only suitable

for small-scale (e.g., <100 kW) PV systems, where the PV array normally interconnects with a low-voltage public network.

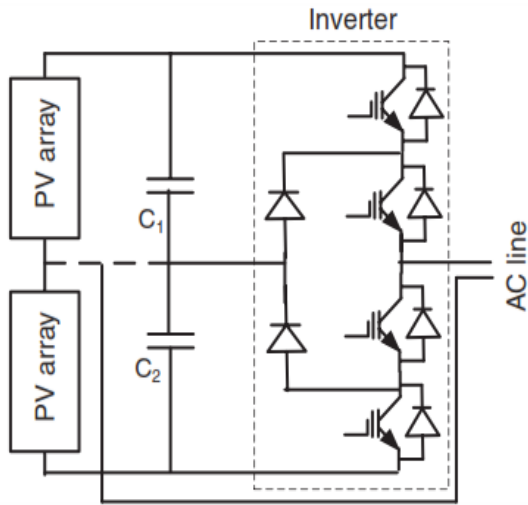


Fig Single-stage power circuit with boost converter [3]

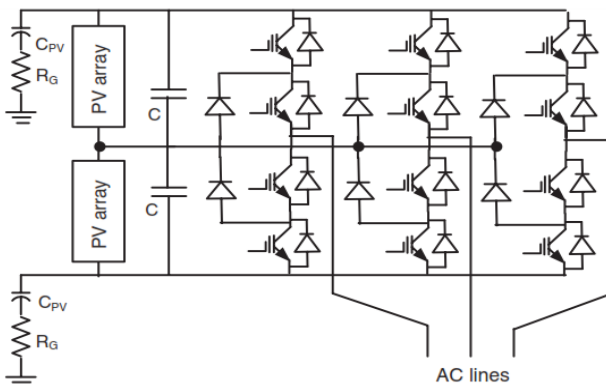


Fig Single-stage power circuit with universal converter [3]

III. RECONFIGURABLE SOLAR CONVERTER

Conventional grid connected inverter uses high dc link voltage, which will be the peak magnitude of the line-line grid voltage [1]. For this particular purpose, two stage conversions are required to boost up the dc voltage and to invert it. However, this will increase the cost, size, and loss of the system. To avoid this, single-phase single-stage topologies of inverter are suggested in [1]–[2]. In the single-phase inverter topology, transformer less inverter gained significant research interest as suggested in [1]. Transformer less inverter has the advantage of low size and cost by avoiding the transformer but this will eliminate the galvanic isolation and inverter will become very sensitive to grid disturbances. The solar PV is limited by its inherent intermittency aspects and, hence, battery storage (assumed here) is required to supply the power when there are not enough solar radiations. But having a separate converter for battery’s power management system will increase the cost and size of the converter as well. Hence, a three-phase topology of reconfigurable solar inverter is introduced in [1] and [2] for utility PV system with battery storage. This reconfigurable system is suitable to solar and wind farm

applications. This topology is tested with a new algorithm and validated the results. Normally, every solar powered household has a battery system to provide a reliable supply system. These batteries are charged when connected to an ac system or they need a separate converter to manage the charging operations when it is connected to the dc supply side.

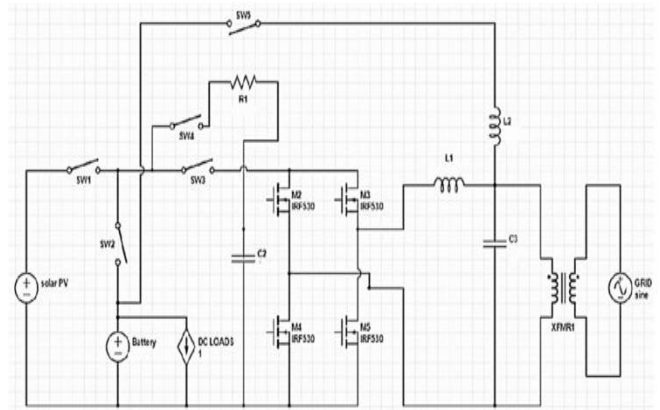


Fig. 4.1 Schematic of the proposed RSC circuit [1]

Therefore, the main contribution of this paper is to implement single-phase single-stage solar converter called reconfigurable solar converter (RSC) in the solar powered hybrid ac/dc residential building with energy storage devices. The basic concept of the RSC is to use a single power conversion system to perform different operational modes such as solar PV to grid (Inverter operation, dc–ac), solar PV to battery/dc loads (dc–dc operation), battery to grid (dc–ac), battery/PV to grid (dc to ac) and Grid to battery (ac–dc) for solar PV systems with energy storage. This inverter is tested in a solar powered hybrid ac/dc home, which contains both ac and dc household loads. Individual appliances are selected according to the harmonic contribution they are injecting to the distribution grid from a typical modern house. Apart from the aforementioned, other additional contributions are as follows. The electrical components and sensors are different from [1], and normal inductor only used for dc/dc operation. The variation in solar radiation is also considered and solar PV-battery operation is verified. The circulation current is mitigated due to operation of the switches in the topology for dc/dc operation. Control logic and sampling of input quantities are also different in this paper.

Modes of operation	ON switches	Off switches
PV-GRID	SW1 SW3 SW 4	SW2 SW 5
PV-BATTERY-GRID	SW1 SW2 SW3 SW4	SW5
PV- BATTERY	SW1 SW3 SW5	SW2 SW4
BATTERY-GRID	SW2 SW3	SW1 SW4 SW5

Table 4.1 Modes of Operation

IV. CONTROL OF THE PROPOSED CONVERTER

For controlling this proposed single-phase inverter, PQ controllers are used considering the advantage that it will

control the active and reactive power according to the reference signal. Since the controlling elements for the ac system are very difficult due to their time-varying nature, the ac control variables are converted to a stationary reference frame from a rotating reference frame for effective control [1].

Let F_{β} be the rotating reference frame variables, which can be voltage or current, whereas F_d and F_q stationary variables. In rotatory reference frame, the active and reactive powers can be calculated by using

$$P = \frac{1}{2} [v_d \times i_d + v_q \times i_q] \dots(1)$$

$$Q = \frac{1}{2} [v_d \times i_q - v_q \times i_d] \dots(2)$$

Where v and i are the instantaneous values of voltage and current, respectively.

When the inverter is synchronized to the grid, the value of v_{β} becomes 0, and (1) and (2) becomes

$$P = \frac{1}{2} [v_d \times i_d] \dots(3)$$

$$Q = \frac{1}{2} [v_d \times i_q] \dots(4)$$

The active and reactive reference currents are given in (5) and (6) as

$$\hat{i}_d = \frac{2 \times \hat{P}}{v_d} \dots(5)$$

$$\hat{i}_q = \frac{2 \times \hat{Q}}{v_d} \dots(6)$$

Where P and Q are the reference power signals of active and reactive power, respectively.

Calculated values of \hat{i}_d and \hat{i}_q are converted into stationary reference frame and given as signal to PQ controller to produce reference signals for the sinusoidal pulse width modulation controller. Synchronizing the solar inverter with grid requires the knowledge of the magnitude and phase of the grid supply voltage. Phase lock loop (PLL) will track the phase of the grid and help to synchronize with the grid. To obtain maximum power from the solar panel, according to maximum power transfer theorem, the panel resistance should be equal to the load resistance, which is connected to this panel. To achieve this, a hill climbing MPPT algorithm is used. This technique will equalize the resistances and extract maximum power from the solar panel.

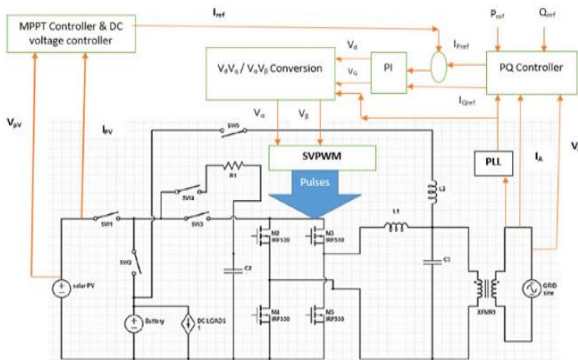


Fig. 4.2 DC/AC inverter operation [1]

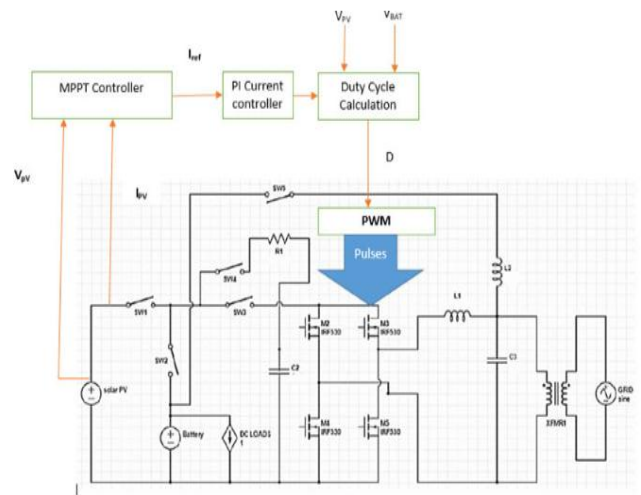


Fig. 4.3 DC/DC chopper operation [1]

The control diagram for different modes of operations of the RSC is given in Figs. 4.2 and 4.3. In Fig. 4.2, the inverter operation of the RSC is explained. From voltage and current measurement from the solar panel, voltage is set to extract maximum power from the panel using MPPT algorithm. This voltage is compared with the set dc-link voltage and error is given to a PI controller for DC link voltage regulation. This PI controller will produce reference current, which is compared with reference current produced using PQ controller, which is given in (5) and (6). This error is given to a PI controller, which will generate reference voltage for active power control. Reactive power is separately controlled using another PI controller. These reference voltages are converted to rotating reference frame voltages and given to space vector pulse width modulation (PWM) to drive the inverter.

V. MODELLING AND SIMULATION

A 30 KW panel is considered as consisting of 24,080 solar cells arranged in 344X70 combinations. The solar array consists of number of panels connected in series-parallel configuration and a panel consists of number of cells. The power characteristics of the solar cell are formulated using its equivalent circuit. The equivalent circuit of the cell is presented as a current source in parallel with diode and a parallel resistance with a series resistance [6].

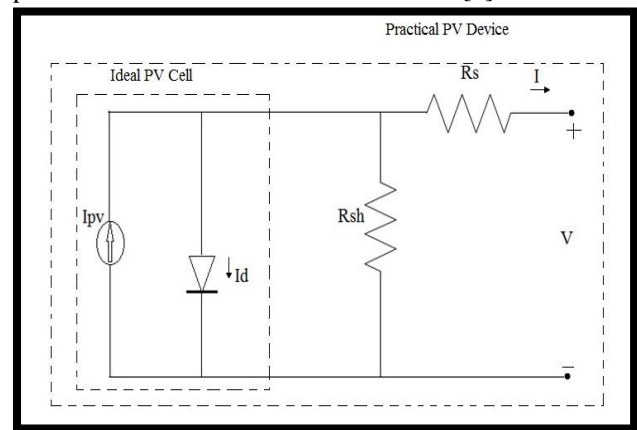


Fig. 6.1: Equivalent circuit of a practical PV device

The output current can be measured by subtracting the diode currents and current through resistance from the light generated current. From this circuit, the output current of the cell is expressed as,

$$I = I_{pv} - I_d - I_{Rsh} \tag{1}$$

$$I = I_{pv} - I_0 \left[\exp\left(\frac{V+IR_s}{a}\right) - 1 \right] - \left(\frac{V+IR_s}{R_p}\right) \tag{2}$$

Where, $a = \frac{NS.A.K.Tc}{q} = Ns.A.V_T$

$$\frac{I_{sc} + K_v * dT}{\exp\left(\frac{V_{oc} + K_v * dT}{a * V}\right) - 1}$$

Where, ns are numbers of cells connected in series. The output current of the solar panel is I. The light generated current is I_{pv} . Saturation currents through diodes are I_0 . The voltage at output of panel is V Series resistance of cell is R_s which represents the internal resistance of cell and it is considered as 0.55Ω . The Boltzmann's constant is K (1.38×10^{-23} J/K). Ambient temperature (in Kelvin) is T and charge constant is q (1.607×10^{-19} C).

A 30 KW solar-PV array is realized considering 24,080 cells (344×70 dimensions) using (1)-(2). A Matlab model for the same is developed.

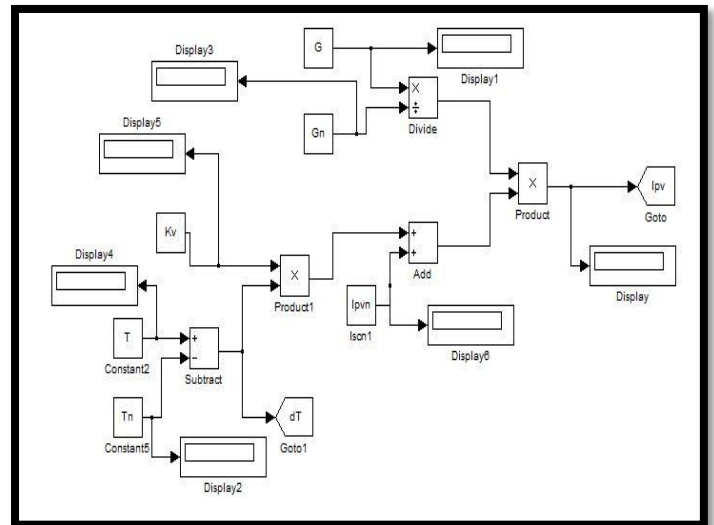


Fig 6.4 Modelling of I_{pv} Current Equation

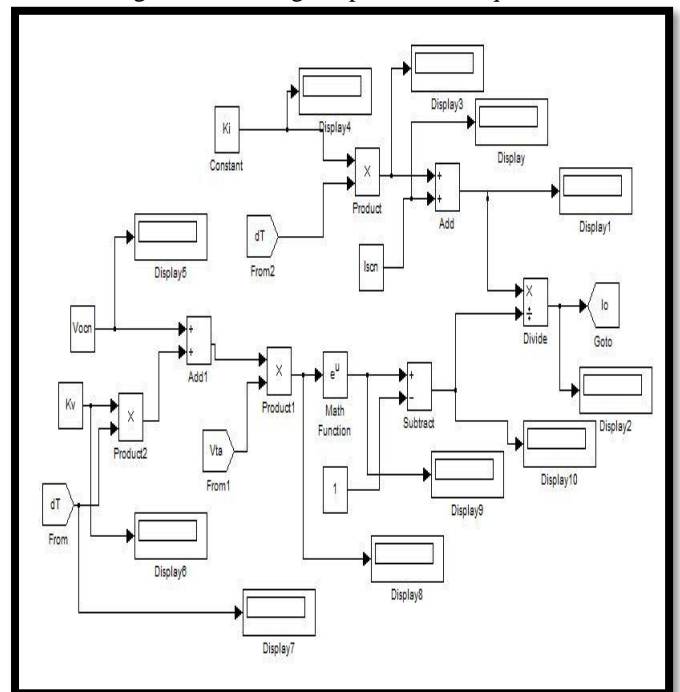


Fig 6.5 Modelling of I_o Current Equation

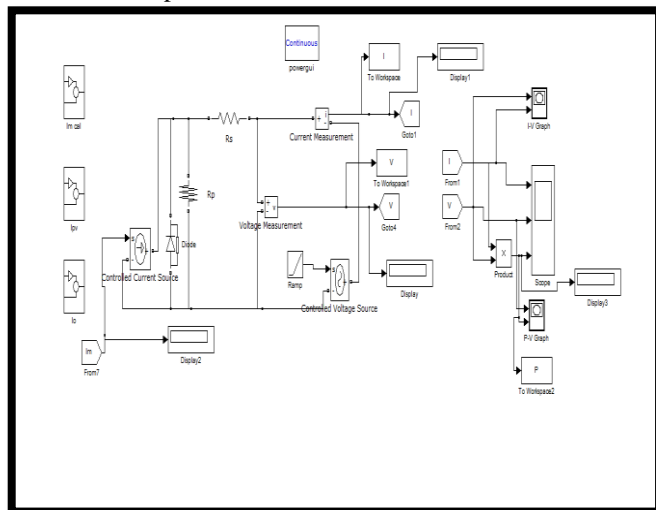


Fig 6.2: Simulink model of a PV device

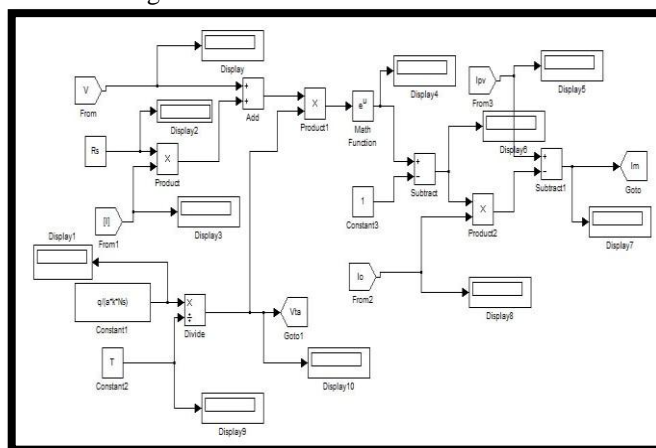


Fig 6.3 Modeling of I_m Current Equation

Table 6.1: Parameters of the PV module at $25^{\circ}C$, $1000 W/m^2$ [6]

I_{mp}	2.88 A
V_{mp}	17 V
P_{mp}	49 W
I_{sc}	3.11 A
V_{oc}	21.8 V
R_s	0.55Ω
K_v	-72.5×10^{-3} V/K
K_i	1.3×10^{-3} A/K
N_s	36

VI. RESULTS

After the simulation, we obtained the following results, Simulation Results of solar panel

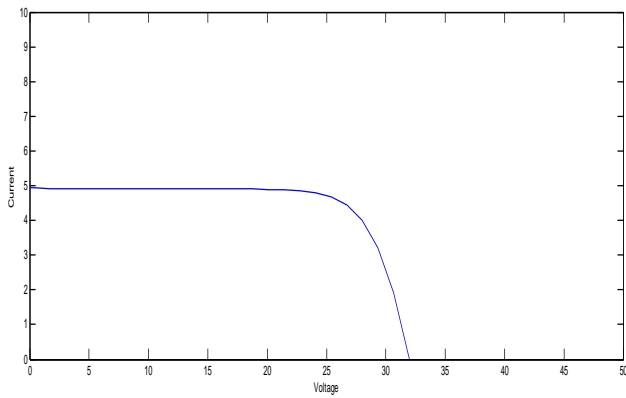


Fig 6.6-I-V Characteristic

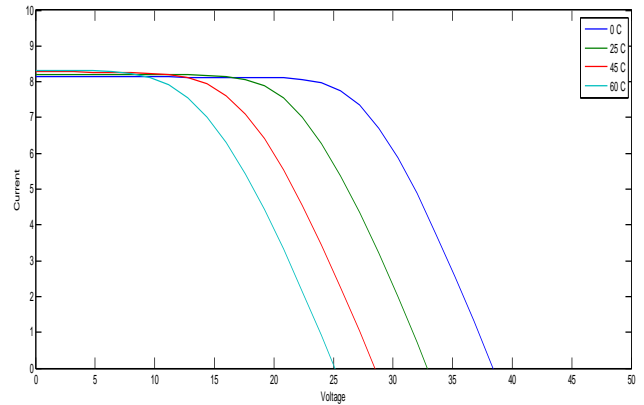


Fig 6.10-Different Temperature I-V Characteristic

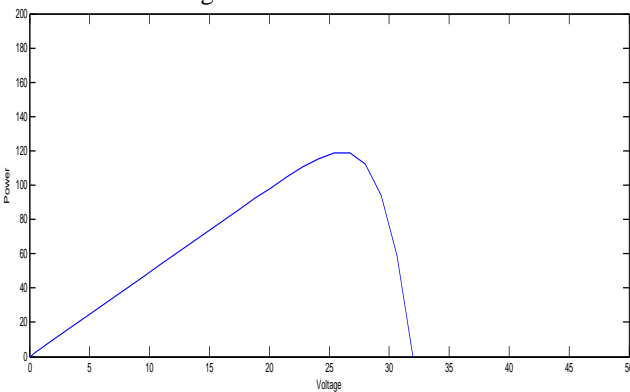


Fig 6.7-P-V Characteristic

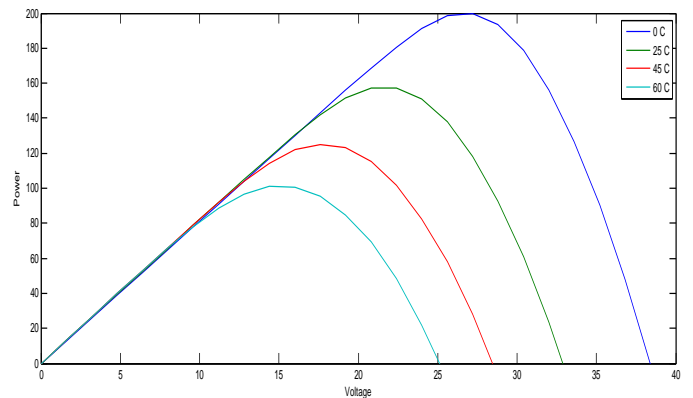


Fig 6.11-Different Temperature P-V Characteristic

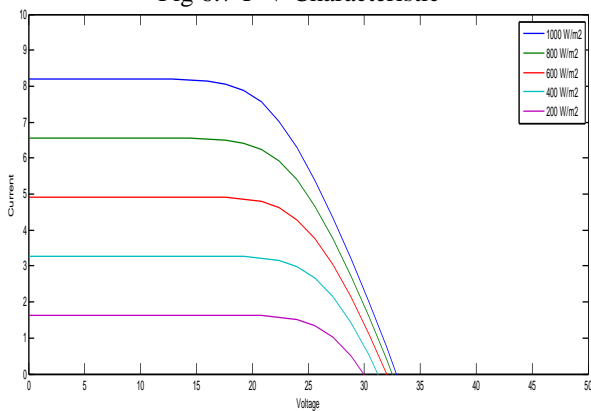


Fig 6.8-Different Radiation I-V Characteristic

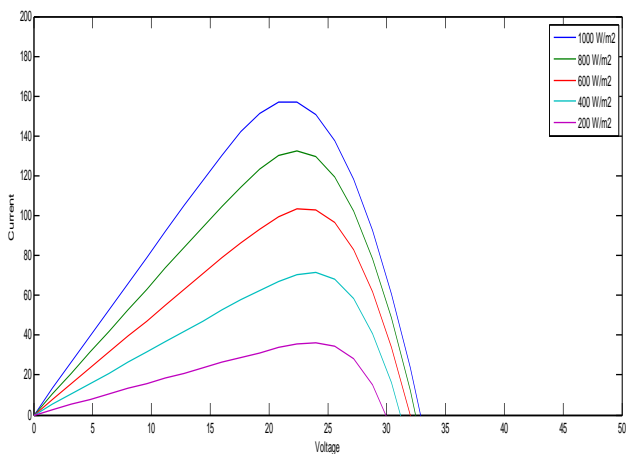


Fig 6.9-Different Radiation P-V Characteristic

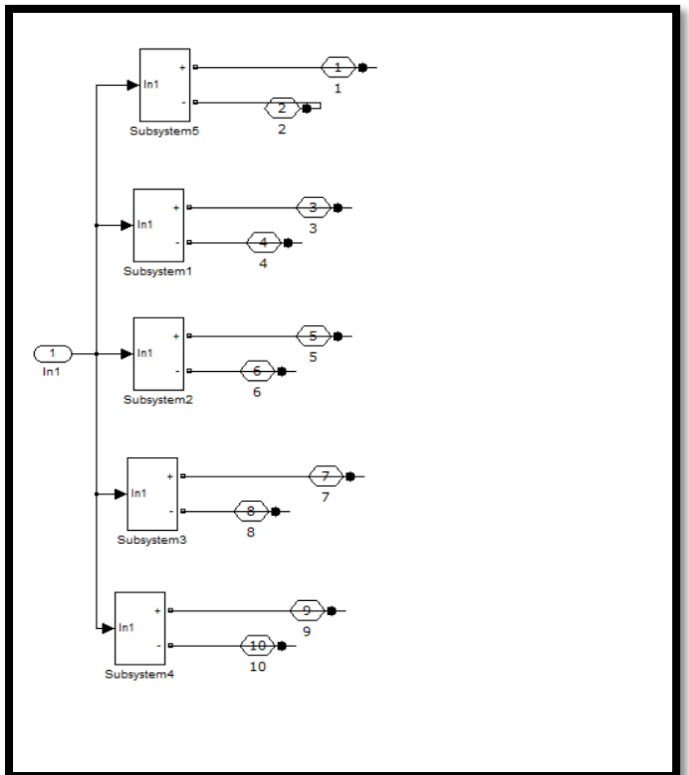


Fig 6.12 Solar PV Array

VII. SOLAR PV SYSTEM WITH MPPT AND BOOST CONVERTER

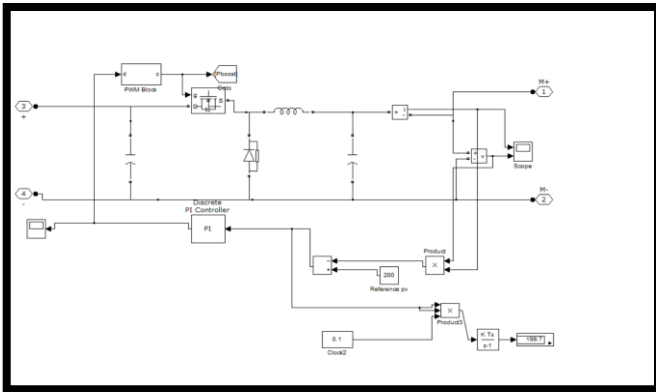


Fig 6.13 Solar MPPT and Boost converter System

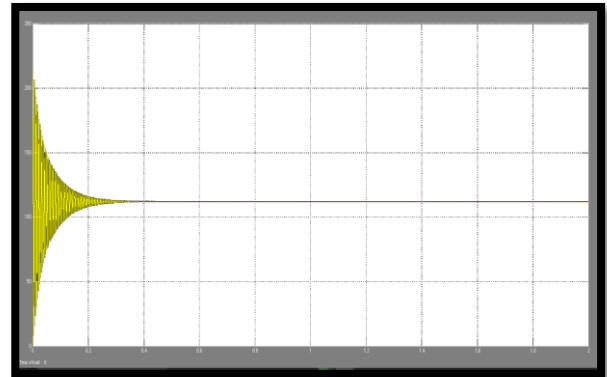


Fig 6.17 Solar D.C stable Output

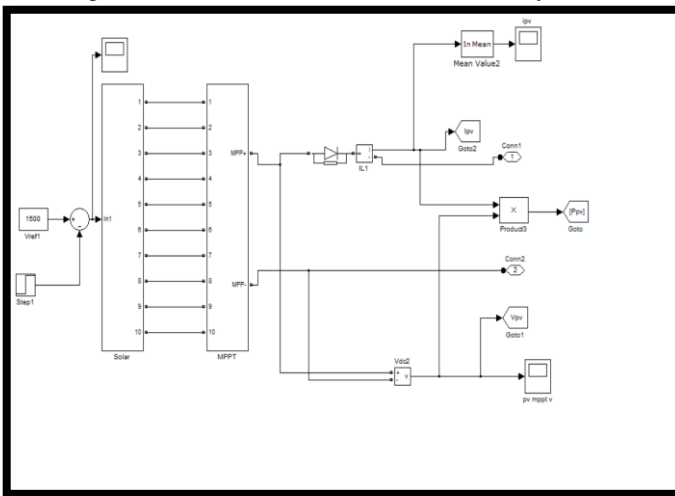


Fig 6.14 Solar PV array and MPPT

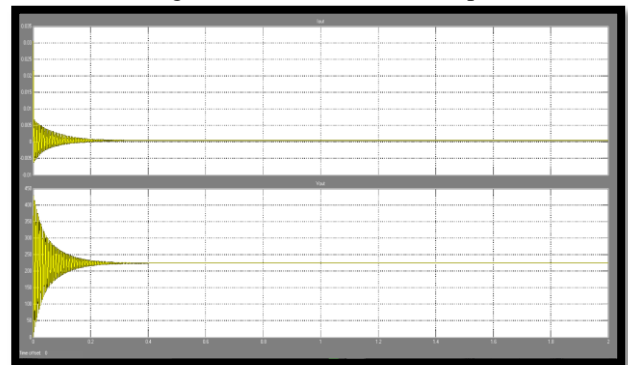


Fig 6.18 Stable output for Solar with MPPT

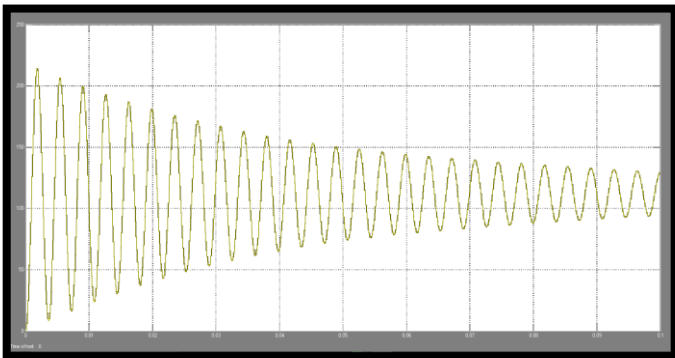


Fig 6.15 Solar Unstable D.C Output



Fig 6.19 D.C Link Capacitor Voltage

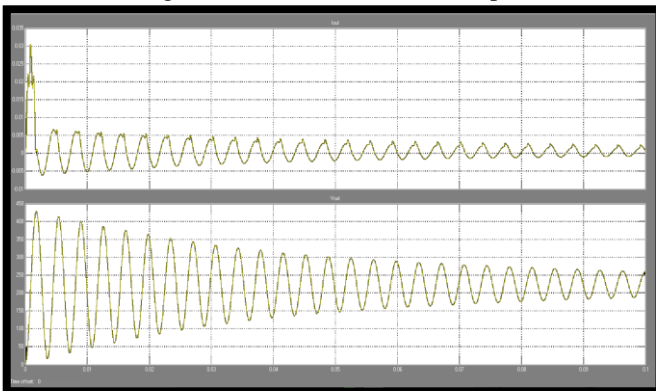


Fig 6.16 Solar Unstable Output

VIII. CONCLUSION

As shown in the graph the P-V and I-V characteristics of PV system changes as per the change in temperature as well as irradiation. So, the PV Generation is very sensitive to any change in the value of temperature as well as irradiation. So accordingly, the output values of all the components connected will be directly affected to this variation. To achieve maximum power point, we can control the current or regulate the voltage to maintain the power. In the proposed system, MPPT regulates the duty cycle to maintain voltage and achieve maximum power. This paper also highlights the future developments, which have the potential to increase the economic attractiveness of such systems and their acceptance by the user. This paper also represents the modelling and Simulation of Solar PV System using MATLAB-

SIMULINK software. The Simulation results show the ideal I-V and P-V characteristics of the solar PV system.

REFERENCES

- [1] Renewables 2014 Global Status Report. REN21. [Online]. Available: <http://www.ren21.net/Portals/0/documents/Resources/GSR/2014/GSR2014full%20report%20low%20res.pdf>
- [2] S. Munir and L. Y. Wei, "Residential distribution system harmonic compensation using PV interfacing inverter," *IEEE Trans. Smart Grid*, vol. 4, no. 2, pp. 816–827, Jun. 2013.
- [3] J. Von Appen, T. Stetz, M. Braun, and A. Schmiegel, "Local voltage control strategies for PV storage systems in distribution grids," *IEEE Trans. Smart Grid*, vol. 5, no. 2, pp. 1002–1009, Mar. 2014.
- [4] A. Arancibia, K. Strunz, and F. Mancilla-David, "A unified single- and three-phase control for grid connected electric vehicles," *IEEE Trans. Smart Grid*, vol. 4, no. 4, pp. 1780–1790, Dec. 2013.
- [5] B. T. Patterson, "DC, come home: DC microgrids and the birth of the enernet," *IEEE Power Energy Mag.*, vol. 10, no. 6, pp. 60–69, Nov./Dec. 2012.
- [6] V. Vossos, K. Garbesi, and H. Shen, "Energy savings from direct-DC in U.S. residential buildings," *Energy Buildings*, vol. 68, no. Part A, pp. 223–231, Jan. 2014.
- [7] N. Sasidharan, N. M. M., J. G. Singh, and W. Ongsakul, "An approach for an efficient hybrid AC/DC solar powered Homegrid system based on the load characteristics of home appliances," *Energy Buildings*, vol. 108, pp. 23–35, Dec. 1, 2015.
- [8] B. Mariappan, B. G. Fernandes, and M. Ramamoorthy, "A novel singlestage solar inverter using hybrid active filter with power quality improvement," in *Proc. 40th Annu. Conf. IEEE Ind. Electron. Soc.*, Oct. 29, 2014–Nov. 1, 2014, pp. 5443–5449.
- [9] C.-M. Wang and C.-H. Yang, "A novel high input power factor soft switching single-stage single-phase AC/DC/AC converter," in *Proc. IEEE Conf. Veh. Power Propulsion*, Sep. 7–9, 2005, p. 5.
- [10] K. M. Shafeeque and P. R. Subadhra, "A novel single-phase single-stage inverter for solar applications," in *Proc. 3rd Int. Conf. Adv. Comput. Commun.*, Aug. 29–31, 2013, pp. 343–346.